

# Pilot-Scale Demonstration of the OSCAR Process for High-Temperature Multipollutant Control of Coal Combustion Flue Gas, Using Carbonated Fly Ash and Mesoporous Calcium Carbonate

Himanshu Gupta,<sup>†</sup> Theodore J. Thomas,<sup>†</sup> Ah-Hyung A. Park,<sup>†</sup> Mahesh V. Iyer,<sup>†</sup> Puneet Gupta,<sup>†</sup> Rajeev Agnihotri,<sup>†</sup> Raja A. Jadhav,<sup>†</sup> Harold W. Walker,<sup>‡</sup> Linda K. Weavers,<sup>‡</sup> Tarunjit Butalia,<sup>‡</sup> and Liang-Shih Fan<sup>\*,†</sup>

Department of Chemical and Biomolecular Engineering, The Ohio State University, 140 W. 19th Avenue, Columbus, Ohio 43210 and the Department of Civil and Environmental Engineering and Geodetic Science, The Ohio State University, 470 Hitchcock Hall, 2070 Neil Avenue, Columbus, Ohio 43210

A pilot-scale study of the Ohio State Carbonation Ash Reactivation (OSCAR) process was performed to demonstrate the reactivity of two novel calcium-based sorbents toward sulfur and trace heavy metal (arsenic, selenium, and mercury) capture in the furnace sorbent injection (FSI) mode on a 0.365 m<sup>3</sup>/s slipstream of a bituminous coal-fired stoker boiler. The sorbents were synthesized by bubbling CO<sub>2</sub> to precipitate calcium carbonate (a) from the unreacted calcium present in the lime spray dryer ash and (b) from calcium hydroxide slurry that contained a negatively charged dispersant. The heterogeneous reaction between these sorbents and SO<sub>2</sub> gas occurred under entrained flow conditions by injecting fine sorbent powders into the flue gas slipstream. The reacted sorbents were captured either in a hot cyclone (~650 °C) or in the relatively cooler downstream baghouse (~230 °C). The baghouse samples indicated ~90% toward sulfation and captured arsenic, selenium and mercury to 800 ppmw, 175 ppmw and 3.6 ppmw, respectively.

## 1. Introduction

Existing and forthcoming regulations could increase the number of sulfur control systems installed on utility power generating units in the United States.<sup>1</sup> Traditionally, utilities have selected between compliance fuel usage (fuel switching to lower sulfur Western coals) and flue gas desulfurization (FGD) installations to meet sulfur emission regulations. Compliance fuel is used by about 70% of the coal-fired power plants, whereas ~22% use FGD systems.<sup>2</sup> Although the number of fossil-fueled steam-electric generators has increased from 1330 units (a capacity of 376.8 GW) in 1993 to 1536 units (a capacity of 409.7 GW) in 2004, the number of FGD installations have increased at a higher rate, from 154 (a capacity of 71.1 GW) to 248 (a capacity of 101.5 GW) over the same period.<sup>3</sup> The implementation of SO<sub>2</sub> control on coal-fired power plants has spanned several decades. Although over 15 different processes could be used to reduce SO<sub>2</sub> emission from power plants,<sup>4,5</sup> wet scrubbing continues to dominate FGD installations. In this process, an aqueous slurry of calcium-based sorbents (calcium hydroxide/carbonate) reacts with SO<sub>2</sub>, producing calcium sulfite. Sulfite is then converted to sulfate through a subsequent forced oxidation step. Another method of the FGD technology is the furnace sorbent injection (FSI). In the FSI process, fine calcium carbonate particulates are injected in the upper furnace region of hot flue gas (800–1000 °C), where they react with SO<sub>2</sub>, producing calcium sulfate.<sup>4</sup>

Economic analyses, based on the EPRI GS-7193 model,<sup>4</sup> conducted on various FGD processes, indicated that wet scrubbing entails a high capital cost, because it necessitates dedicated equipment, and its implementation in retrofit applica-

tions is potentially hindered by its large footprint. However, the conversion of calcium-based sorbents to CaSO<sub>3</sub>/CaSO<sub>4</sub> is high, as measured by the molar ratio of calcium injected to sulfur captured (Ca/S ratio = 1.05–1.1). This high calcium conversion leads to a lower levelized cost for SO<sub>2</sub> emissions reduction. In contrast, the capital cost associated with furnace sorbent injection (FSI) is low and is more amenable for retrofitting due to its smaller footprint. However, FSI leads to a higher levelized cost, because of the lower calcium utilization (Ca/S ratio = 2–4). A sorbent capable of higher reactivity under FSI conditions could potentially achieve the desirable combination of the low sorbent requirement of wet scrubbing and the low capital cost of FSI. This study was conducted to demonstrate the performance of two high-reactivity calcium-based sorbents on a pilot scale.

The Ohio State Carbonation Ash Reactivation (OSCAR) process<sup>6</sup> was invented and developed from initial fundamental research to the current stage of pilot demonstration. The OSCAR process potentially has major advantages over the traditional FGD technologies. These include lower capital costs, lower fresh sorbent requirements, more retrofit opportunities, and lesser byproduct generation which could lead to lower disposal costs. In addition, the formation of CaSO<sub>4</sub>, and not CaSO<sub>3</sub> (as in the lower temperature processes), coupled with the much lower content of free calcium in the form of CaO enables the potential use of OSCAR byproducts in the cement industry. Calcium-based sorbents also capture trace heavy metals that are included in the EPA's list of 189 hazardous pollutants included in Title III of the Clean Air Act Amendments<sup>7</sup> of 1990. Arsenic, which poisons NO<sub>x</sub>-reducing selective catalytic reduction (SCR) catalysts,<sup>8</sup> and selenium react with calcium oxide to form thermally stable calcium arsenate and selenite, respectively, at medium temperatures (400 – 600 °C).<sup>9–11</sup> Calcium-based sorbents also reduce lead and cadmium from flue gas streams at temperatures in the range of 500–800 °C.<sup>12–14</sup> The beneficial role of the higher surface area of these sorbents on arsenic capture has also been demonstrated at laboratory scale.<sup>15</sup>

\* To whom correspondence should be addressed. Tel.: (614) 688-3262. Fax: (614) 292-3769. E-mail address: fan.1@osu.edu.

<sup>†</sup> Department of Chemical and Biomolecular Engineering.

<sup>‡</sup> Department of Civil and Environmental Engineering and Geodetic Science.

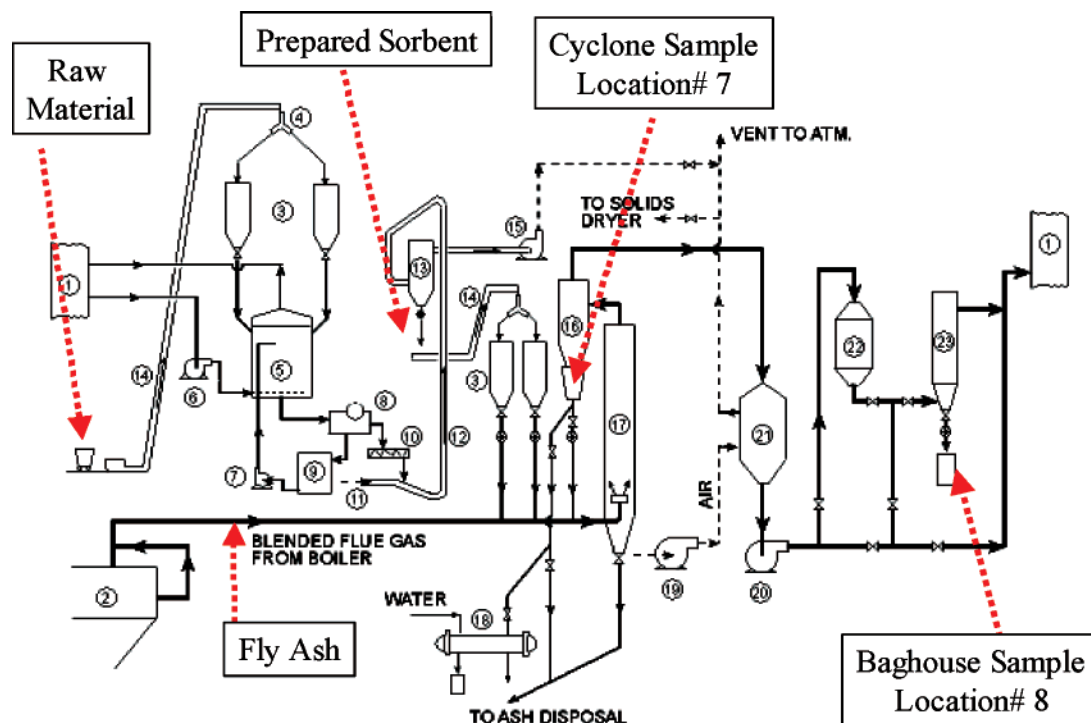


Figure 1. Schematic of the OSCAR flow diagram and sampling locations for solid samples.

Based on previous reaction kinetic and mechanistic studies and patents,<sup>6,16–18</sup> the OSCAR process was installed downstream from the coal-fired boiler at the McCracken Power Plant located at The Ohio State University (OSU) and demonstrated on a pilot-scale. This paper focuses on the sulfur and trace metals capture capabilities of these two sorbents.

## 2. Experimental Section

**2.1. Sorbent Preparation. 2.1.1. Sorbent A: Carbonation of Spent Lime Spray Dryer Ash.** In a relatively lower-temperature lime spray dryer (LSD) process used for the reduction of  $\text{SO}_2$  from flue gas, calcium hydroxide ( $\text{Ca}(\text{OH})_2$ ) particles are injected into the cooler section of the flue gas duct, where it captures  $\text{SO}_2$  in the form of calcium sulfite/sulfate. Under these operating conditions, some calcium remains unreacted (in the form of oxide/hydroxide). During hydration of the spent LSD ash, water reacts with the unreacted  $\text{CaO}$  core,<sup>19</sup> which is encapsulated by the product layer of calcium sulfite, to form  $\text{Ca}(\text{OH})_2$ . Calcination of the  $\text{Ca}(\text{OH})_2$ , upon its reinjection at high temperatures encountered in the FSI mode, further increases the porosity and provides additional reactive  $\text{CaO}$  surface for  $\text{SO}_2$  gas. Hydration<sup>20</sup> increases the utilization of spent sorbent, from 35% up to 70% and attains an overall molar ratio of  $\text{Ca}/\text{S}$  (calcium injected to sulfur captured) of  $\sim 2.4$ .

In comparison, one of the OSU patents<sup>16</sup> accomplishes the regeneration of spent LSD ash by bubbling  $\text{CO}_2$  through an aqueous slurry of the spent LSD ash to convert unreacted calcium into  $\text{CaCO}_3$ . Combined with reactivation of unreacted  $\text{CaO}$ , this process also provides a better distribution/exposure of available calcium<sup>20,21</sup> than the reactivated spent sorbent from hydration alone. The LSD ash indicated a conversion of 38% that was increased to 65% by hydration and 85% by carbonation. This process formed the heart of the OSCAR process.

**2.1.2. Sorbent B: Reengineered Precipitated Calcium Carbonate (PCC).** The high-temperature heterogeneous sulfation reaction between  $\text{SO}_2$  and calcium-based sorbents that occurs in the upper furnace region in FSI mode is characterized

by two regimes. The kinetically controlled regime<sup>9</sup> occurs first in which the reaction proceeds as a result of direct interaction between the  $\text{CaO}$  surface and gaseous  $\text{SO}_2$  forming a continuous, smooth, nonporous layer of calcium sulfate, a higher molar volume product than calcium carbonate/oxide. This product layer completely surrounds the reactive core of  $\text{CaO}$  particles, thereby making the  $\text{SO}_2$  gas inaccessible to the  $\text{CaO}$  at the reacting front. Further reaction progresses in the second ionic diffusion controlled regime in which metal ions diffuse through this product layer to the reaction front. This regime progresses at a relatively slower rate than the kinetic regime.<sup>22</sup>

Micropores ( $<5$  nm in diameter) that dominate the porosity in calcined natural limestone present the second hurdle to high solid conversion during sulfation reaction due to their susceptibility to pore mouth closure and pore pluggage, as a result of the formation of higher-molar-volume  $\text{CaSO}_4$ . Here, the surface area across which the sulfation reaction could proceed is limited. Therefore, a typical once-through system such as the FSI process requires 3 or 4 mol of calcium per mole of sulfur<sup>4</sup> to be removed to achieve a sulfur removal level exceeding 50%.

Prior research<sup>9,23,24</sup> has shown that particles that are dominated by mesopores (5–20 nm) attain a much higher conversion to sulfation. A patented precipitation process,<sup>6,15,20,21</sup> which involves bubbling  $\text{CO}_2$  gas through a negatively charged dispersant-modified  $\text{Ca}(\text{OH})_2$  slurry, has yielded mesoporous  $\text{CaCO}_3$  particles (also called supersorbent in this manuscript) that demonstrate an almost 3-fold improvement in reactivity toward sulfation. The OSCAR project is undertaken to demonstrate the performance of these two sorbents on a pilot scale by simulating FSI conditions on a slipstream of OSU's McCracken Power Plant Boiler No. 8, which utilizes high-sulfur Ohio coal.

**2.2. Pilot-Scale OSCAR Testing System.** The layout of the OSCAR testing system is presented in Figure 1. Overall, the OSCAR process consists of two sections: the cold section, which is used to synthesize these two sorbents, and the hot section, which is used to test the reactivity of the sorbents. In the following sections, the numbers in parentheses represent

the equipment identified in Figure 1, not the references listed at the end of the manuscript.

**2.2.1. Cold Section.** A metal screw conveyor (14) moves the raw materials from the receiver hopper to the two upper hoppers (3). The raw materials were then metered into a slurry reactor (5), in which the carbonation of the free calcium occurs using the CO<sub>2</sub> in the flue gas of the main power plant. The carbonation<sup>18</sup> was a batch process and a substantial change in the pH of the solution from ~12 to ~6 indicates a complete conversion of calcium to CaCO<sub>3</sub>. The slurry was dried to 40 wt % water content using a vacuum drum filter (8) and to 10 wt % in a heated twin screw conveyor (10). This sorbent powder is completely dried by a portion of the hot air, detailed later in this section, separated from it in a bag filter (13). Another metallic conveyor (14) moved the now-dried sorbents to hoppers (3), where a set of rotary valves injected these sorbent particles into the flowing hot flue gas for each testing.

**2.2.2. Hot Section.** The hot section of the OSCAR system begins at the boiler taps (2) of the OSU's McCracken Power Plant No. 8 boiler, which uses bituminous coal. Sorbent particles were metered from two storage hoppers (3) into this flue gas stream, which was followed by the mixture entering the straight riser section. The riser reactor (17), 8 m in height and 0.61 m in diameter, was designed to provide a nominal residence time of 1.6 s. The gas and solids exiting the top of the riser reactor enter a cyclone (16), where sorbent particles were separated from the gas stream based on particle size. The predicted cyclone efficiency was 96.8% at full load with a pressure drop of 1.4 kPa at a nominal flow of 0.365 m<sup>3</sup>/s. The receiver at the bottom of the cyclone was equipped with a 0.1-m flanged solids outlet to route the hot sorbent particles to a water-cooled thin-film paddle-type ash cooler (18). The flue gas exiting the cyclone was cooled from 790 °C to 370 °C by raising the temperature of the ambient air to 230 °C in a gas–gas heat exchanger (21). A portion of the hot, ambient air is used to dry the wet sorbent particles exiting the heated twin-screw conveyor. The cooled flue gas now enters a variable-speed induced-draft (ID) fan (20) that controlled the gas flow rate through the entire slipstream. This 37-kW motor-driven fan was capable of moving up to 0.51 m<sup>3</sup>/s gas at 370 °C at a differential pressure of 8.34 kPa.

Downstream from the ID fan, the gas flow was split into two streams, representing 30% and 70% of the main flue gas flow. The 30% stream (~0.11 m<sup>3</sup>/s) flows through a selective catalytic reduction (SCR) unit (22) and a downstream baghouse (23), which collects finer sorbent particles that escaped the hot cyclone. A lower flow rate through the baghouse was necessary to minimize the footprint of the baghouse unit. The two streams recombine downstream of the bag filter, before joining the main power plant flue gas duct (1) before the lime spray dryer unit of the McCracken Power Plant.

**2.2.3. List of Solid Samples and Sampling Locations Employed in the Pilot Unit.** Many types of solids were involved in the OSCAR process. This section briefly defines and describes the various solid samples and their sampling locations.

**Boiler Fly Ash:** Boiler fly ash is fly ash collected from McCracken boiler No. 8 without any injection of calcium-based sorbents. This mixture is typical of fly ash generated from a stoker-fired coal combustion unit.

**LSD Ash:** The main McCracken power plant applies a lime spray dryer (LSD) using hydrated lime slurry to reduce SO<sub>2</sub> emissions. The solids exiting the LSD are called LSD ash. It consists of fly ash and a mixture of reacted and unreacted calcium compounds including calcium hydroxide and calcium

**Table 1. Operational Parameters for the Pilot-Scale OSCAR Demonstration**

run	reaction temperature [°C]	flue gas flow rate, through cyclone [m <sup>3</sup> /h]	sorbent injection rate [kg/h]	sorbent type
1	681	7544	27	sorbent A
2	642	7773	77	sorbent A
3	642	7391	56	sorbent A
4	650	7527	44	sorbent A
5	653	7433	8	sorbent A
8	645	4757	18	sorbent A
31	643	8325	16	sorbent B
32	643	8325	23	sorbent B
33	639	7306	4	sorbent B
34	629	5267	16	sorbent B
35	640	8359	16	sorbent B
37	646	5479	16	sorbent B
38	673	5055	16	sorbent B
39	660	4587	10	sorbent B

sulfite. The two samples were collected from sampling locations 7 and 8, shown in Figure 1.

**Regenerated OSCAR Sorbent (Sorbent A):** This is the sorbent made by carbonating the LSD ash to regenerate the unreacted calcium in the slurry reactor.

**Supersorbent (Sorbent B):** Supersorbent is mesoporous calcium carbonate made from pure hydrated lime (see section 2.1.2). The two sorbents can be collected from the storage bin under the baghouse (13).

**Cyclone Samples (Run 7):** The larger size fraction of any entrained solids was collected in the bin under the cyclone (16) at location 7. These samples are referred to as Run 7.

**Baghouse Samples (Run 8):** The finer solid particles that escape the cyclone are collected in the baghouse (location 8). These samples are referenced as Run 8.

**2.2.4. Test Matrix.** This demonstration project successfully completed 21 experimental runs on the OSCAR testing system. The run numbers and the experimental conditions used in each run are provided in Table 1. The single-digit numbered experiments were performed with the regenerated OSCAR sorbent (Sorbent A) and the experimental runs with numbers in the 30s were performed with the supersorbent (Sorbent B). An attempt was made to study the effect of reaction temperature and residence time on the reactivity of these two sorbents. However, the temperature effect could not be completed, because of the inability to achieve a flue gas temperature exceeding 700 °C. This was much lower than the temperature range used in previous laboratory experiments that have been reported by the authors (900–1100 °C).<sup>15</sup> Thus, all the experiments were performed at the highest temperature attained by the flue gas in a particular run. The typical residence time in commercial FSI operation is in the range of 0.3–1.5 s. A similar exposure time range was attained in this pilot project by varying the flue gas flow rate. For example, Run 4A was conducted at a total gas flow rate of 2009 kg/h, whereas Run 8A was conducted at 1270 kg/h, an increase in residence time of ~57%.

### 3. Results and Discussion

The experimental results obtained in this study are separately discussed for the regenerated OSCAR sorbent (Sorbent A) and supersorbent (Sorbent B). In each case, the prepared sorbent and the resulting reaction product were examined using a battery of analytical tools, including SediGraph5100 (manufactured by Micromeritics) for particle size distribution and scanning electron microscopy (SEM) for surface morphology. Surface and pore properties of samples were determined using N<sub>2</sub> adsorption on a Brunauer–Emmett–Teller (BET) apparatus



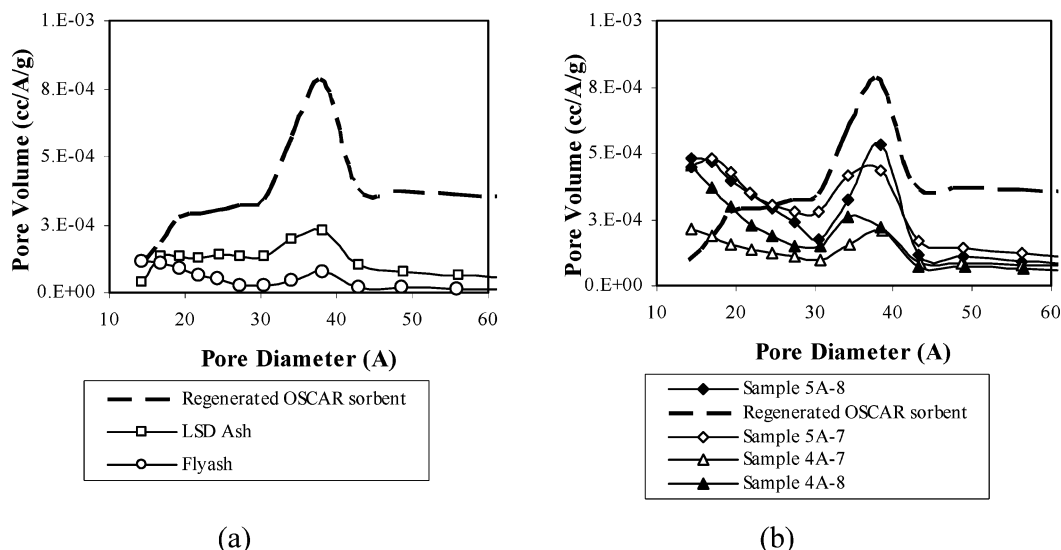


**Figure 2.** Pore size distributions of the OSCAR sorbent (sorbent A), compared to (a) the starting materials and (b) its reaction products.

**Table 2.** Morphological Characteristics of Solid Samples Obtained from the OSCAR Regenerated Sorbent (Sorbent A) Testing

solid sample	BET Surface Area [m <sup>2</sup> /g]		pore volume [mL/g]
	1 point	n point	
fly ash	7.27	7.51	0.005788
LSD ash	8.87	9.11	0.01960
regenerated OSCAR sorbent	35.40	36.62	0.08412
run-location			
4A-7	23.56	24.17	0.03439
4A-8	32.80	33.68	0.03146
5A-7	29.00	30.20	0.04078
5A-8	29.53	30.47	0.03313
8A-7	38.76	39.70	0.02783

(Model NOVA 2200, Quantachrome, Inc.). The concentration of sulfate ions was established via ion chromatography (IC) and the elemental analysis was conducted on an inductively coupled plasma–optical emission spectrometry (ICP–OES) system. X-ray diffractometry (XRD) was used to elucidate the crystal structures of the inorganic solid compounds.

### 3.1. Regenerated OSCAR Sorbent Testing: Sorbent A.

**3.1.1. Physical Characterization of Sorbent A and Its Reaction Products.** The morphological properties of the regenerated OSCAR sorbent prepared for this study are provided in Table 2, and the pore size distributions of typical solid samples are compared in Figure 2. The surface area and pore volume of the fly ash were low, amounting to only 7.51 m<sup>2</sup>/g and 0.006 mL/g, respectively. It is possible that the presence of high-porosity unburnt carbon in fly ash enhanced the measured surface area and pore volume. The product exiting the main power plant's lime spray dryer unit (called LSD ash) also showed low porosity. This was due to the fact that the hydrated lime was partially converted to a larger molar volume product, CaSO<sub>3</sub>, as a result of its reaction with SO<sub>2</sub>, under LSD conditions. This reaction product also contains the entrained low-porosity fly ash. In contrast, carbonation of the regenerated OSCAR sorbent leads to a significant increase in surface area and pore volume, because of the formation of a higher-porosity precipitated calcium carbonate (PCC) from the unreacted calcium hydroxide during the carbonation process (Figure 2a).

Upon the injection of the regenerated OSCAR sorbent into the riser reactor and its subsequent sulfation, two solid samples were collected in the cyclone and the baghouse to be analyzed. Despite a slight variation in the porosities of the two samples observed during Run 4, a consistent difference was not supported by the data obtained from other experimental runs. As evident

from Figure 2b, the sulfation reaction, which caused the buildup of a higher-molar-volume product (CaSO<sub>4</sub>) compared to the starting material (CaCO<sub>3</sub>), resulted in a decline in the porosity of the sorbent particles. This phenomenon was also supported from the data in Table 2, which showed that the surface area and pore volume of both solid samples collected at the cyclone and the baghouse were lower than those of the unreacted OSCAR sorbent. The decrease in porosity after sulfation can also be partially attributed to the dilution of reacted sorbent with relatively nonporous fly ash in the riser reactor.

The particle size distributions of the solid samples are shown in Figure 3. The average particle size of the LSD ash was 33 μm, whereas the average particle size of the regenerated OSCAR sorbent was 22 μm. This was due to finer particles of CaCO<sub>3</sub> forming upon regeneration. After SO<sub>2</sub> removal in the riser reactor, the cyclone captures the bulk of the sorbent particles (>90%). The particle size distribution of the cyclone samples (Run–Location sample 4A–7) is similar to the regenerated OSCAR sorbent. The solid sample captured in the baghouse showed a much narrower range of the particle size as evident in Figure 3. The average particle size of the reacted sorbent captured in the baghouse was 5 μm. The SEM photomicrograph shown in Figure 4, shown at the same magnification, visually confirm measured particle sizes.

### 3.1.2. Sulfur Capture Using Regenerated OSCAR Sorbent.

All the solid samples collected during the operation of the OSCAR process were subjected to XRD analysis for crystal structure identification. Table 3 lists all the crystal structures associated with the sorbent samples collected in this project. Table 3 shows that fly ash contains typical mineral matter components, such as SiO<sub>2</sub>, Fe<sub>2</sub>O<sub>3</sub>, and Al<sub>2</sub>SiO<sub>5</sub>. The LSD ash contained both unreacted Ca(OH)<sub>2</sub> and reacted product,

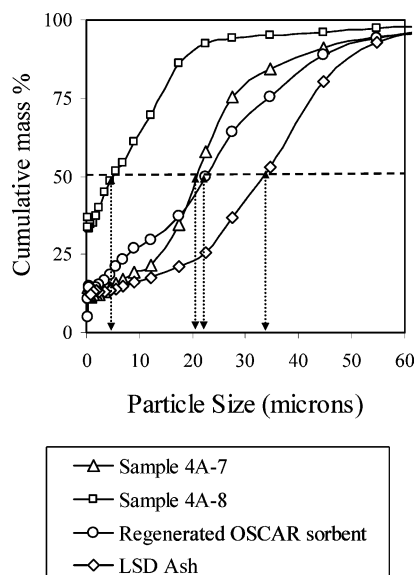


**Figure 3.** Particle size distributions of the OSCAR sorbent (sorbent A), compared to the McCracken Power Plant lime spray dryer (LSD) and its reaction products (legend: run–location).

$\text{CaSO}_3 \cdot \frac{1}{2}\text{H}_2\text{O}$  in comparable quantities. The XRD analysis of the regenerated OSCAR sorbent, made by carbonating unreacted calcium in LSD ash, demonstrates complete conversion of the unreacted  $\text{Ca}(\text{OH})_2$  to  $\text{CaCO}_3$ , as indicated by the absence of peaks corresponding to the structure of  $\text{Ca}(\text{OH})_2$ . It was also found that  $\text{CaSO}_3 \cdot \frac{1}{2}\text{H}_2\text{O}$  in the LSD ash remains intact in the regenerated OSCAR sorbent.

The XRD patterns of the reacted OSCAR sorbent captured in the cyclone are dominated by  $\text{CaCO}_3$ . This is due to the lower apparent conversion of the cyclone sample, the reasons for which will be detailed later. The only sulfur-containing structure in the baghouse sample of the reacted OSCAR sorbent was  $\text{CaSO}_4$ , whereas there was no trace of  $\text{CaSO}_3 \cdot \frac{1}{2}\text{H}_2\text{O}$ . This is one of the previously mentioned advantages of the OSCAR process. Although the sulfur-containing structure in LSD ash is  $\text{CaSO}_3 \cdot \frac{1}{2}\text{H}_2\text{O}$ , which needs to be oxidized in a subsequent step, the OSCAR byproduct contains  $\text{CaSO}_4$ , which does not need further treatment before its disposal. The XRD analysis of the baghouse sample did not show any other crystal structure, indicating the possibility of a very high conversion to sulfation of calcium in this fine particulate sample.

The results of the chemical analysis performed on these sorbent samples using ICP and IC techniques are given in Table 4. According to the ICP results, the calcium content of the fly ash was expectedly low, because fly ash from Ohio coals are known to contain only small quantities of alkaline-earth metals. However, the LSD ash was rich in calcium, because of the use of hydrated lime during the LSD process. The weight percent of calcium in the regenerated OSCAR sorbent is lower than that of LSD ash, because, as calcium carbonate (MW = 100 g/mol) was formed from the calcium hydroxide (MW = 74 g/mol), more mass was added to the solid sample without any addition of calcium.

For a comparison of sulfur capture by calcium, it is more meaningful to express it in terms of the ratio of the captured sulfur to calcium (S/Ca) in the solid sample. For example, in pure calcium sulfate, the ratio would be 32/40 (i.e., 0.8). In LSD ash, this ratio was 0.41, which decreased to 0.36 after the reactivation process based on carbonation reaction. Higher values of the S/Ca ratio were expected for the solids samples

collected from both the cyclone and the baghouse, because they were the products of the sulfation reaction. The S/Ca ratio of the baghouse samples was indeed higher, thereby ascertaining that the sorbent did capture a significant amount of sulfur in the flue gas stream. However, the S/Ca ratio in the cyclone samples was determined to be <0.36 for both Runs 4A and 8A, being 0.30 and 0.34, respectively. The decrease in the S/Ca ratio of the cyclone sample could be due to a variety of reasons. Thermodynamically,  $\text{CaSO}_3 \cdot \frac{1}{2}\text{H}_2\text{O}$  could oxidize to  $\text{CaSO}_4$  or thermally decompose to  $\text{CaO}$  and  $\text{SO}_2$  gas. However, if oxidation of the  $\text{CaSO}_3 \cdot \frac{1}{2}\text{H}_2\text{O}$  were occurring, some  $\text{CaSO}_3 \cdot \frac{1}{2}\text{H}_2\text{O}$  could potentially remain in the cyclone sample, because of incomplete oxidation. Although the exact kinetics of the oxidation reaction are not known, it is reasonable to believe that the probability of complete oxidation is low. In contrast, the complete absence of peaks corresponding to the XRD pattern of  $\text{CaSO}_3 \cdot \frac{1}{2}\text{H}_2\text{O}$  and a noticeable increase in the  $\text{SO}_2$  concentration in the flue gas upon the injection of the regenerated OSCAR sorbents into the riser reactor support the complete decomposition of  $\text{CaSO}_3 \cdot \frac{1}{2}\text{H}_2\text{O}$ . After decomposition, the  $\text{CaO}$  can react with both the  $\text{SO}_2$  produced due to the calcium sulfite decomposition and the  $\text{SO}_2$  present in the flue gas due to the combustion of high-sulfur coal. The low conversion of  $\text{CaO}$  toward sulfation (as shown in the cyclone samples) suggest that, under the process conditions in the riser, the kinetics of decomposition of calcium sulfite is rapid but that of  $\text{CaO}$  sulfation are slow. A higher temperature and longer residence time would have enabled a high conversion. For example, the Ca/S ratio of Run–Location samples 4A-7 and 8A-7 samples indicate that the Ca/S ratio increases from 0.3 to 0.34 as the residence time increases by 57% (see Table 4).

While the cyclone captures the relatively larger particles, the finer particles continue reacting with  $\text{SO}_2$  gas at higher temperatures for a longer time and are then collected at a cooler temperature ( $\sim 230^\circ\text{C}$ ). The average solid residence time of the baghouse sample is  $\sim 1$  min instead of 1.6 s of exposure time of the cyclone sample in the riser reactor. XRD data in Table 3 show that  $\text{CaSO}_4$  dominates the baghouse solid sample, indicating a high reactivity and yield of the sulfation reaction. In addition, according to the ICP analysis presented in Table 4, the S/Ca ratio of the baghouse sample for Runs 4A and 8A were 0.59 and 0.85, respectively. The high S/Ca ratio of the baghouse sample for Run 8A indicates >90% conversion of calcium, which is a significant milestone of this project. While baghouse samples collected in Runs 4A and 8A were exposed for similar duration at the lower baghouse temperatures, this sample traveled through the higher-temperature portion of the flue gas duct for a longer time, because of the lower flue gas flow rate in Run 8A. This indicates that the residence time associated with the higher-temperature region near the riser reactor has a more significant effect on the overall sulfur capture than longer exposure at lower temperature.

The IC results were analyzed to ascertain the chemical form of sulfur in various samples. It was difficult to quantify sulfite ions in an IC column, as it underwent partial oxidation during analysis, which is an unavoidable consequence of the analytical technique. This creates uncertainty in determining the sulfate content of the LSD ash and the regenerated OSCAR sorbent. However, the sulfate analysis of the cyclone and baghouse samples may be considered accurate based on the XRD analysis. IC results corroborate the ICP findings that, although the cyclone samples were similar in sulfur capture for Runs 4A and 8A, there was a distinct increase in the sulfur capture of the baghouse sample in Run 8A, compared to Run 4A.

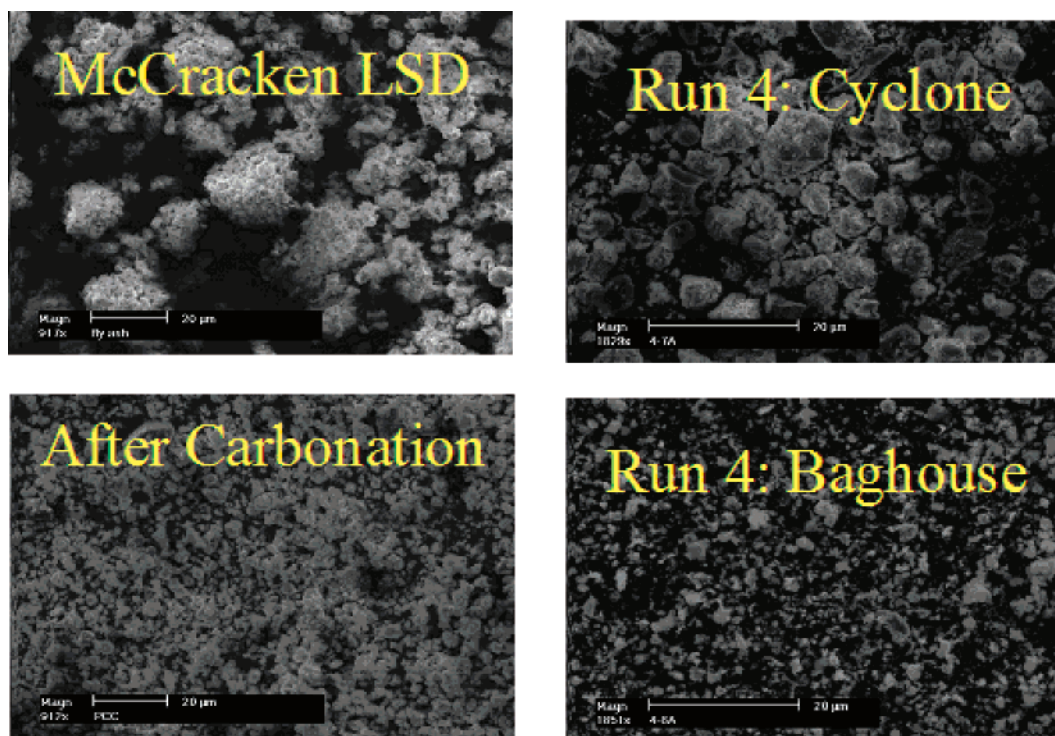


Figure 4. Scanning electron microscopy (SEM) photomicrographs of solid samples collected during the regenerated OSCAR sorbent testing.

Table 3. Summary of Crystal Structures in Various Solid Samples Identified by X-ray Diffractometry (XRD)

sample	sorbent sample	main inorganic crystal structures
1	fly ash	SiO <sub>2</sub> , Fe <sub>2</sub> O <sub>3</sub> , and Al <sub>2</sub> SiO <sub>5</sub>
2	LSD ash	Ca(OH) <sub>2</sub> , CaSO <sub>3</sub> · $\frac{1}{2}$ H <sub>2</sub> O, SiO <sub>2</sub> ,
3	regenerated OSCAR sorbent	CaCO <sub>3</sub> , CaSO <sub>3</sub> · $\frac{1}{2}$ H <sub>2</sub> O, SiO <sub>2</sub> ,
4	cyclone sample from regenerated OSCAR sorbent experiment	CaCO <sub>3</sub> , CaSO <sub>4</sub> , CaO, SiO <sub>2</sub>
5	baghouse sample from regenerated OSCAR sorbent experiment	CaSO <sub>4</sub> , CaO, CaCO <sub>3</sub>
6	cyclone sample from supersorbent experiment	CaCO <sub>3</sub> , CaSO <sub>4</sub> , SiO <sub>2</sub>
7	baghouse sample from supersorbent experiment	CaSO <sub>4</sub>

Table 4. ICP/IC Analysis of Solid Samples Obtained from the Regenerated OSCAR Sorbent (Sorbent A) Testing

	Starting Material		Sorbent	Run—Location Sample			
	fly ash	LSD ash		regenerated OSCAR sorbent	4A-7	4A-8	8A-7
ICP Results							
calcium (wt %)	0.42	32	23	15	17.6	15.5	12.6
sulfur (wt %)	0.4	13	8.3	4.5	10.4	5.3	10.7
mercury (mg/kg)	UDL <sup>a</sup>	0.46	0.50	<0.05	3.6	<0.05	2.6
arsenic (mg/kg)	69.3	32	56.2	80.1	501.7	90.8	569.9
selenium (mg/kg)	8.2	28	22.8	22.4	144.4	23.3	168.8
S/Ca ratio	0.95	0.41	0.36	0.30	0.59	0.34	0.85
IC Results							
sulfate (wt %)	0.05	28.2	14	10.7	22.7	11.9	40.3
sulfur (wt %)	0.02	9.40	4.67	3.57	7.57	3.97	13.43

<sup>a</sup> Undetectable level.

**3.1.3. Arsenic and Selenium Capture Using Regenerated OSCAR Sorbent.** Regenerated OSCAR sorbent was also very efficient in capturing trace heavy metals. According to the ICP analysis, the arsenic and selenium content of the fly ash sample were ~69.3 and ~8.2 mg/kg, respectively. The arsenic content was even lower in the LSD ash, because the hydrated lime probably has a lower arsenic content. A similar trend was not observed for selenium, because the selenium content of the LSD ash is higher. The regeneration of the LSD ash through carbonation led to an increase in the arsenic concentration and a decrease in selenium concentration. The reasons for this trend are not apparent. However, because “cold” flue gas was used as a source of CO<sub>2</sub> gas during the carbonation process, it is possible that the heavy metals present in the vapor phase of the

flue gas may have condensed on the solid particles upon contact with the water in the slurry reactor. ICP data presented in Table 4 do not show a significant increase in the arsenic and selenium capture by the cyclone samples. However, the baghouse samples showed a dramatic rise in both arsenic and selenium concentrations, to 502–570 mg/kg and 144–169 mg/kg, respectively.

It is interesting to note that the arsenic capture in the baghouse sample was higher than both the cyclone samples and the LSD ash. LSD ash sample was exposed to flue gas only at low temperature and the cyclone sample was in contact with flue gas only at high temperatures. Previous experimental data indicate an optimum reaction temperature to be ~500 °C for the maximum reactivity of calcium to arsenic.<sup>25</sup> The high capture of arsenic in the baghouse sample confirms the laboratory



**Table 5. Morphological Characteristics of Solid Samples Obtained from the Supersorbent (Sorbent B) Testing**

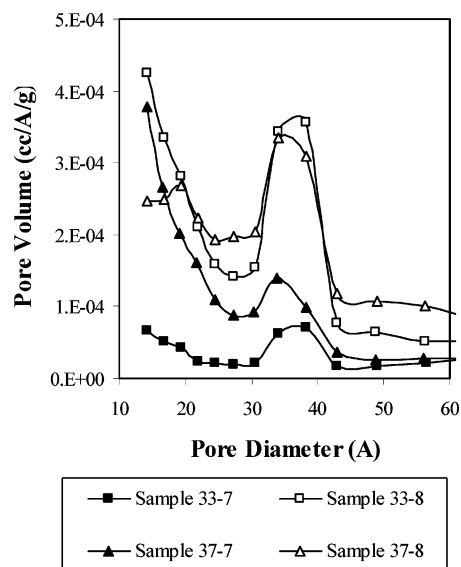
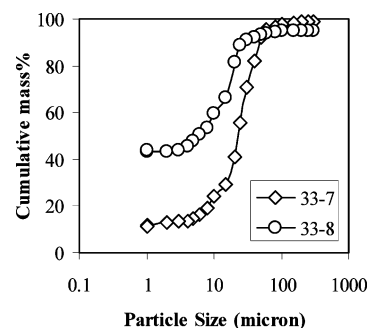
solid sample	BET Surface Area [m <sup>2</sup> /g]		pore volume [mL/g]
	1 pint	n pint	
fly ash	7.27	7.51	0.005788
LSD ash	8.87	9.11	0.01960
super sorbent	35.40	36.62	0.08412
run—location			
33—7	10.41	10.16	0.01990
33—8	32.36	33.33	0.03678
37—7	25.64	27.34	0.01849
37—8	24.19	24.45	0.02756

finding, because only the particles collected in the baghouse sample come into contact with the flue gas in the optimum temperature range for calcium—arsenic interaction.

**3.1.4. Mercury Capture Using Regenerated OSCAR Sorbent.** The trend in mercury concentration was slightly different. While there was no mercury detected in the fly ash sample, LSD ash measured 0.46 mg/kg of mercury in its solid sample. There are two potential sources of mercury in LSD ash. Either hydrated lime inherently had some mercury, or the LSD operation at OSU's McCracken Power Plant led to the capture of mercury by calcium to some degree. After carbonation, which was conducted by cooler flue gas, the mercury content of the regenerated OSCAR sorbent showed a slight increase to 0.5 mg/kg. This addition may also have occurred from the mercury in flue gas binding to calcium/sulfur in the sorbent in the carbonation slurry reactor.

The injection of the regenerated OSCAR sorbent into the riser reactor led to a drop in the mercury level in the cyclone samples from both Runs 4A and 8A to below the detection limit of the instrument (i.e., 0.05 mg/kg). Apparently, under the high temperature of the riser reactor, the mercury evolution rate from the regenerated OSCAR sorbent was higher than the mercury capture rate. On the other hand, the baghouse sample showed a significant amount of mercury capture, reaching as high as 2.6–3.6 mg/kg, probably because of the higher residence time at the relatively lower temperature in the baghouse. Mercury capture by the regenerated OSCAR sorbent is similar to the mercury capture level attained by other calcium-based sorbents.<sup>26–29</sup> For example, HCl-treated calcium-based sorbents such as hydrated lime captures 0.108 mg/kg Hg<sup>0</sup> and calcium sulfate captures 2.27 mg/kg from a 32-ppb mercury-containing gas stream. The beneficial effect of 500 ppmv SO<sub>2</sub> at 100 °C in a 40 ppb mercury stream is apparent from the increase in the elemental mercury sorption capacity of hydrated lime<sup>27</sup> from 1 mg/kg to 2.5 mg/kg. Although we did not actively measure mercury concentration in the flue gas slipstream, the mercury capture by the regenerated OSCAR sorbent seems to be comparable to literature studies. Calcium-based sorbents still have lower mercury adsorption capacities and reactivity than the high-surface-area activated carbons that have been traditionally used.<sup>27</sup> However, the cost of the calcium-based sorbents is only a fraction of that of activated carbons, and because multipollutant control (i.e., SO<sub>2</sub>, arsenic, selenium, and mercury) can be achieved, mercury removal using calcium-based sorbents becomes very attractive. Therefore, the OSCAR process may provide an inexpensive alternative as a multipollutant control system with a single, low-cost calcium-based sorbent.

**3.2. Precipitated Calcium Carbonate (PCC) Testing: Sorbent B. 3.2.1. Physical Characterization of Sorbent B and Its Reaction Products.** The surface area and pore volume of the samples collected from the supersorbent testing are listed in Table 5. Conversion of the solids to form higher-molar-volume products and the capture of lower-porosity fly ash

**Figure 5.** Pore size distributions of the reaction products of the supersorbent (sorbent B) (legend: run—location).**Figure 6.** Particle size distributions of the reaction products of the supersorbent (sorbent B) collected in the hot cyclone and the baghouse (legend: run—location).

combine to reduce the porosity of both the cyclone and baghouse samples, compared to the porosity of the supersorbent. BET analyses indicate a higher pore volume of the baghouse samples over that of the cyclone samples. Run 37 was conducted by injecting sorbent into the riser reactor at a rate that is 4 times higher than for Run 33. It is possible that, for the same residence time and reactor temperature, the conversion of the supersorbent in Run 37 may not be as high as that in Run 33. This might explain the lower drop in porosity of the cyclone and baghouse samples. The pore size distribution, shown in Figure 5, indicates that the porosity of the baghouse samples for Runs 33 and 37 was higher than that of the cyclone samples, in agreement with data presented in Table 5.

The particle size distribution for the cyclone and baghouse samples collected from Run 33 is shown in Figure 6. As expected, the cyclone sample was much larger than the baghouse sample, with the medium size of 20  $\mu\text{m}$  and 5.4  $\mu\text{m}$ , respectively. As discussed earlier, with respect to the regenerated OSCAR sorbent testing, in addition to the effects of residence time and reaction temperature, this drastic difference in particle size could also explain the higher conversion observed of the baghouse sorbent, compared to the solid sample collected at the cyclone. Previous laboratory testing<sup>20</sup> indicates that there is an almost 2-fold decrease in reactivity as the particle size becomes larger than 3.9  $\mu\text{m}$ .

**3.2.2. Sulfur and Trace Metal Capture Using PCC.** The high purity of the hydrated lime used to synthesize supersorbent was confirmed using thermogravimetric analysis (TGA). In an

**Table 6. ICP/IC Analysis of Solid Samples Collected in the Hot Cyclone from the Supersorbent (Sorbent B) Testing**

			Run—Location							
	lime	supersorbent	31—7	32—7	33—7	34—7	35—7	37—7	38—7	39—7
ICP Results										
calcium (wt %)	53.51	32.30	7.61	24.50	24.62	26.97	29.87	19.03	23.68	23.56
sulfur (wt %)	0.04	2.05	1.00	1.76	1.75	2.45	2.20	1.42	2.52	3.28
mercury (mg/kg)	UDL <sup>a</sup>	2.1	0.46	UDL <sup>a</sup>	UDL <sup>a</sup>	UDL <sup>a</sup>	UDL <sup>a</sup>	UDL <sup>a</sup>	UDL <sup>a</sup>	UDL <sup>a</sup>
arsenic (mg/kg)	UDL <sup>a</sup>	5.9	73	52	43	58	38	72.8	52.3	55.3
selenium (mg/kg)	UDL <sup>a</sup>	UDL <sup>a</sup>	UDL <sup>a</sup>	0.7	2.3	2.0	UDL <sup>a</sup>	UDL <sup>a</sup>	UDL <sup>a</sup>	UDL <sup>a</sup>
lead (mg/kg)	16	14	47	29	33	22	23	27	20	20
polyaromatic hydrocarbons, PAHs (ppb)			38	169	167	203	177	116	123	84
S/Ca ratio	0.00	0.06	0.13	0.07	0.07	0.09	0.07	0.07	0.11	0.14
IC Results										
sulfate (wt %)			2.3	3.56	6.22	17.95	3.44	2.01	5.00	4.28
sulfur (wt %)			0.77	1.19	2.07	5.98	1.15	0.67	1.67	1.43

<sup>a</sup> Undetectable level.**Table 7. ICP/IC Analysis of Solid Samples Collected in the Baghouse from the Supersorbent (Sorbent B) Testing**

			Run—Location							
	lime	supersorbent	31—8	32—8	33—8	34—8	35—8	37—8	38—8	39—8
ICP Results										
calcium (wt %)	53.51	32.30	7.5	7.5	8.3	8.3	12.4	11.0	15.9	19.6
sulfur (wt %)	0.04	2.05	7.9	7.7	7.6	7.6	7.6	7.9	7.4	7.4
mercury (mg/kg)	UDL <sup>a</sup>	2.1	3.4	3.1	3.6	3.4	2.2	2.4	2.7	2.2
arsenic (mg/kg)	UDL <sup>a</sup>	5.9	798.3	829.9	830.6	823.5	793.1	672.7	583.2	596.4
selenium (mg/kg)	UDL <sup>a</sup>	UDL <sup>a</sup>	166.1	168.4	173.5	154.7	124.2	120.1	117.4	110.3
lead (mg/kg)	16	14	379.4	199.8	202.3	198.5	193.7	142.3	169.2	159.8
polyaromatic hydrocarbons, PAHs (ppb)				490.4	813.7		283.2	305.5	613.2	388.3
S/Ca ratio	0.00	0.06	1.1	1.0	0.9	0.9	0.6	0.7	0.5	0.4
IC Results										
sulfate (wt %)			18.0	19.1	20.1	20.3	20.0	24.4	21.6	24.1
sulfur (wt %)			6.0	6.4	6.7	6.8	6.7	8.1	7.2	8.0

<sup>a</sup> Undetectable level.

inert nitrogen gas flow, the solids mass was reduced by 24.3% at temperatures beyond 700 °C. This is comparable to the theoretical weight loss associated with the conversion of Ca(OH)<sub>2</sub> (MW = 74 g/mol) to CaO (MW = 56 g/mol). ICP data on raw lime in Table 6 indicates a calcium mass of 53.5 wt %, which is similar to the 54.05% mass of calcium that is contained in pure Ca(OH)<sub>2</sub>. As mentioned previously, the conversion of lime to calcium carbonate increases the overall mass of the particles without any addition of calcium, causing the calcium to decrease to 32.3% in the supersorbent. The carbonation process introduces sulfur, arsenic, and mercury to the supersorbent, probably because cold flue gas was used as a source of CO<sub>2</sub>.

Table 6 indicates that the calcium content of all the cyclone samples is reduced, probably because of the addition of low-calcium-containing fly ash. The sulfur capture in the cyclone sample was not significant. This parallels the finding with the regenerated OSCAR sorbent. Similar reasons, consisting of a shorter residence time and lower riser reactor temperature, probably explain the lower sorbent reactivity. Another reason for lower sulfur capture during the pilot-scale testing is the lower concentration of SO<sub>2</sub> in the OSCAR system, which was only ~600–900 ppm, compared to the 3900 ppm used in previous laboratory studies.<sup>15</sup>

In the eight sets of experiments presented in Table 6, the S/Ca ratio for the cyclone samples varied from 0.07 to 0.14, indicating a conversion of 8.8% to 17.5%, with respect to sulfur capture. The IC data, which indicates a conversion range of 5%–27.5%, parallels the ICP data. The XRD data (Table 3) revealed that CaCO<sub>3</sub> was the dominant component in the cyclone sample. The sulfur capture occurs in the form of only CaSO<sub>4</sub>, which has the advantages mentioned in section 3.1.2.

The baghouse sample analyses revealed the most promising data obtained in this pilot-scale demonstration. The data shown in Table 7 indicates that the S/Ca ratio for four out of the eight samples show an almost-complete conversion to sulfate, assuming all the sulfur was bound with calcium. The XRD patterns confirm that the dominant peaks are assigned to CaSO<sub>4</sub>, which indicates very high sulfur capture by calcium. There were much smaller peaks associated with silica, but none with other calcium compounds, notably CaO and CaCO<sub>3</sub>, were observed in the baghouse sample. Hence, it is concluded that the use of supersorbent does not entail the uncertainty associated with the decomposition of CaSO<sub>3</sub>·<sup>1</sup>/<sub>2</sub>H<sub>2</sub>O during the FSI process.

According to the ICP results in Tables 6 and 7, similar to the results obtained for the regenerated OSCAR sorbent, the capture of arsenic and selenium in the cyclone samples was not very significant, probably due to the limited residence time and the high reaction temperature. Arsenic and selenium captures were observed to be in the ranges of 38–117 mg/kg and <2.3 mg/kg, respectively. However, the capture of trace heavy metals by calcium was remarkable in the baghouse samples. Although the capture of selenium amounted to 110–173 mg/kg, the arsenic uptake by supersorbent was even higher than that of the regenerated OSCAR sorbent, resulting in a range of 580–830 mg/kg. Reacted supersorbent samples collected at the baghouse location also indicated a mercury capture of 2.2–3.6 mg/kg. These capture data are less than the previous laboratory data of arsenic capture by calcium under differential fixed-bed conditions (in the 1800–6000 mg/kg range).<sup>25</sup> However, the pilot-scale OSCAR demonstration results are very promising, considering that the laboratory results were obtained using an inlet concentration of arsenic (i.e., 14 ppm) that was much higher than that of typical flue gas.



#### 4. Conclusions

The pilot-scale demonstration study of the Ohio State Carbonation ASH Reactivation (OSCAR) process involved the design, erection, and commissioning of a pilot plant capable of synthesizing sorbent at a rate of 45.4 kg/day to be tested on the flue gas stream of 0.365 m<sup>3</sup>/s. Several analytical tools were used for a comprehensive characterization of the solid samples collected during the operation of the OSCAR system. The sorbent synthesis was successfully scaled-up with desired morphological characteristics. The surface area and pore volume of the regenerated OSCAR sorbent were 35–36 m<sup>2</sup>/g and 0.0841 mL/g, respectively, which are comparable to the sorbent generated at the laboratory scale using pure hydrated lime and CO<sub>2</sub> gas. The XRD analysis confirmed the conversion of all the free calcium remaining in the spent lime spray dryer (LSD) ash to calcium carbonate during the proposed method of regeneration process.

The two sorbents, the regenerated OSCAR sorbent (sorbent A) and the re-engineered precipitated calcium carbonate (PCC) (sorbent B or supersorbent), yielded similar trends in the capture of sulfur and trace metals, when they were injected into the riser reactor in the FSI mode. The results of chemical analyses revealed that both calcium-based sorbents achieved limited conversion by larger sorbent particles collected in the hot cyclone, whereas the finer sorbent particles captured in the baghouse attained near-stoichiometric capacity. The Sedi-Graph5100 analysis revealed that the particle size and its distribution of the solid samples collected in the baghouse were smaller and narrower than those of the cyclone samples. The smaller particle size explained, in part, the higher conversion of calcium toward sulfur and trace heavy metals in the baghouse samples. The higher sulfur capture by the baghouse samples could also possibly be a result of longer residence time for finer sorbent particles throughout the system. During this pilot-scale demonstration, it was found that both the residence time and the reaction temperature also affect the capture of sulfur and trace metals. For both sorbents, the X-ray diffraction (XRD) results ascertained that the only sulfur species present in postreaction samples was CaSO<sub>4</sub>, which allows for disposal in landfills and byproduct utilization, such as its use as a raw material in the cement industry, without the necessity of a forced oxidation step.

Another advantage of the OSCAR process was its capture capability toward trace metals such as arsenic, selenium, and mercury. Negligible concentrations of arsenic, selenium, and mercury were found in the starting raw materials such as LSD ash and hydrated lime. However, after the injection of sorbent A or sorbent B, the arsenic and selenium capture was noticeable in the cyclone samples (in the tens of ppmw) and substantial in the baghouse samples (in the range of hundreds of ppmw). A greater arsenic capture by the finer sorbent particles collected in the baghouse was observed, compared to the samples collected in the cyclone samples. This was because the finer particles were exposed to the optimum temperature of the arsenic capture (~500 °C) for longer periods of time. In addition, significant amounts of mercury were captured by both sorbents, particularly by the regenerated OSCAR sorbent.

#### Acknowledgment

The financial assistance provided by the Ohio Coal Development Office (OCDO) of the Ohio Air Quality Development Authority (OAQDA) in support of this OSCAR process demonstration study is gratefully acknowledged. The authors

would also like to express the appreciation to the following individuals who had assisted in the various aspects of this study: Danold W. Golightly, Ping Sun, Panuwat Taerakul, David Johnson, Jon Harris, Henry Dammeyer, and Wallace Giffen.

#### Literature Cited

- (1) U.S. Department of Energy (DOE) Milliken Clean Coal Demonstration Project: A DOE Assessment, Report DOE/NETL-2001/1156, U.S. Department of Energy, Washington, DC, 2001.
- (2) Berland, T. D.; Pflughoeft-Hassett, D. F.; Dockter, B. A.; Eylands, K. E.; Hassett, D. J.; Heebink, L. V. Review of Handling and Use of FGD Material, Final Report for U.S. Department of Energy, Energy & Environmental Research Center: Grand Forks, ND, April 2003.
- (3) Energy Information Administration (EIA), Steam-Electric Plant Operation and Design Report, Form EIA-767, 2006.
- (4) Electric Power Research Institute (EPRI), Economic Evaluation of Flue Gas Desulfurization Systems, EPRI GS-7193, February 1991.
- (5) Srivastava, P. K. Controlling of SO<sub>2</sub> Emissions: A Review of Technologies, U.S. Environmental Protection Agency Report EPA/600/R-00/093, Office of Research and Development, Washington DC, November 2000.
- (6) Fan, L.-S.; Ghosh-Dastidar, A.; Mahuli, S. Calcium Carbonate Sorbent and Methods of Making and Using Same, U.S. Patent 5,779,464, 1998.
- (7) Environmental Protection Agency (EPA), The original list of hazardous air pollutants, <http://www.epa.gov/ttn/atw/orig189.html>, 2006.
- (8) Valdés-Solís, T.; Marbán, G.; Fuertes, A. B. Low-temperature SCR of NO<sub>x</sub> with NH<sub>3</sub> over carbon-ceramic supported catalysts. *Appl. Catal., B* **2003**, *46*, 261–271.
- (9) Ghosh-Dastidar, A.; Mahuli, S.; Agnihotri, R.; Fan, L.-S. Investigation of High-Reactivity Calcium Carbonate Sorbent for Enhanced SO<sub>2</sub> Capture. *Ind. Eng. Chem. Res.* **1996**, *35* (2), 598–603.
- (10) Mahuli, S.; Agnihotri, A.; Chauk, S.; Fan, L.-S. Mechanism of Arsenic Sorption by Hydrated Lime. *Environ. Sci. Technol.* **1997**, *31*, 3226–3231.
- (11) Agnihotri, A.; Chauk, S.; Mahuli, S.; Fan, L.-S. Selenium Removal Using Ca-Based Sorbents: Reaction Kinetics. *Environ. Sci. Technol.* **1998**, *32*, 1841–1846.
- (12) Uberoi, M.; Shadman, F. Sorbents for removal of lead compounds from hot flue gases. *AIChE J.* **1990**, *36*, 307–309.
- (13) Uberoi, M.; Shadman, F. High-temperature removal of cadmium compounds using solid sorbents. *Environ. Sci. Technol.* **1991**, *25*, 1285–1289.
- (14) Gullett, B. K.; Raghunathan, K. Reduction of Coal-Based Metal Emissions by Furnace Sorbent Injection. *Energy Fuels* **1994**, *8*, 1068.
- (15) Mahuli, S.; Agnihotri, R.; Wei, S.; Chauk, S.; Fan, L.-S. Pore Structure Optimization of Calcium Carbonate for Enhanced Sulfation. *AIChE J.* **1997**, *43* (9), 2323–2335.
- (16) Fan, L.-S.; Mahuli, S.; Agnihotri, R. Suspension Carbonation Process for Reaction of Partially Utilized Sorbent, U.S. Patent 6,309,996 B1, 2001.
- (17) Fan, L.-S.; Jadhav, R. Perspective: Clean Coal Technologies: OSCAR and CARBONOX Commercial Demonstrations. *AIChE J.* **2002**, *48* (10), 2115–2133.
- (18) Fan, L.-S.; Agnihotri, R. Carbonation Ash Reactivation Process and System for Combined SO<sub>x</sub> and NO<sub>x</sub> Removal, U.S. Patent 6,569,388 B1, 2003.
- (19) Couturier, M. F.; Marquis, D. L.; Steward, F. R.; Volmerange, Y. Reactivation of partially-sulphated limestone particles from a CFB combustor by hydration. *Can. J. Chem. Eng.* **1994**, *72*, 91–97.
- (20) Agnihotri, R.; Chauk, S.; Mahuli, S.; Fan, L.-S. Sorbent/Ash Reactivation for Enhanced SO<sub>2</sub> Capture Using Novel Carbonation Technique. *Ind. Eng. Chem. Res.* **1999**, *38* (3), 812–819.
- (21) Jiang, P.; Agnihotri, R.; Chauk, S.; Fan, L.-S. Dispersion and Ultrafast Reaction of Calcium Based Sorbent in a Circulating Fluidized Bed. *Chem. Eng. Sci.* **1999**, *54* (22), 5585–5598.
- (22) Borgwardt, R. H.; Bruce, K. R.; Blake, J. An Investigation of Product-Layer Diffusivity for CaO Sulfation. *Ind. Eng. Chem. Res.* **1987**, *26*(10), 1993–1998.
- (23) Wei, S.-H.; Mahuli, S. K.; Agnihotri, R.; Fan, L.-S. High Surface Area Calcium Carbonate: Pore Structural Properties and Sulfation Characteristics. *Ind. Eng. Chem. Res.* **1997**, *36* (6), 2141–2148.
- (24) Gullett, B. K.; Bruce, K. R. Pore Distribution Changes of Calcium Based Sorbents Reacting with Sulfur Dioxide. *AIChE J.* **1987**, *33* (10), 1719–1726.

- (25) Jadhav, R.; Fan, L.-S. Capture of Gas Phase Arsenic Oxide by Lime: Reaction Kinetics. *Environ. Sci. Technol.* **2001**, *35* (4), 794–799.
- (26) Ghorishi, B.; Gullett, B. K. Sorption of mercury species by activated carbons and calcium-based sorbents: effect of temperature, mercury concentration and acid gases. *Waste Manage. Res.* **1998**, *16* (6), 582–593.
- (27) Ghorishi, S. B.; Sedman, C. B. Low concentration mercury sorption mechanisms and control by calcium-based sorbents: application in coal-fired processes. *J. Air Waste Manage. Assoc.* **1998**, *48*, 1191–1198.
- (28) Ghorishi, B.; Gullett, B. K.; Jozewicz, W.; Kozłowski, W. Role of HCl in Adsorption of Elemental Mercury Vapor by Calcium-based Sorbents, National Technical Information Service (NTIS), Springfield, VA, Publication No. PB99-171548, EPA Report No. 600/A-99/060, 1999.

- (29) Krishnan, S. V.; Bakhteyar, H.; Sedman, C. B. Mercury sorption mechanisms and control by calcium-based sorbents. In *Proceedings of Air & Waste Management Association's 89th Annual Meeting & Exhibition*, Paper No. 96-WP64B.05, Nashville, TN, June 23–28, 1996.

*Received for review* January 14, 2007

*Revised manuscript received* April 30, 2007

*Accepted* May 2, 2007

IE070090H